Journal of Anatomy

J. Anat. (2019) **235**, pp626–636 doi: 10.1111/joa.13018

The total number of white matter interstitial neurons in the human brain

Goran Sedmak[1,2] and Miloš Judaš[1,2]

[1]*Croatian Institute for Brain Research, School of Medicine, University of Zagreb, Zagreb, Croatia*
[2]*Center for Excellence in Basic, Clinical and Translational Neuroscience, Zagreb, Croatia*

Abstract

In the adult human brain, the interstitial neurons (WMIN) of the subcortical white matter are the surviving remnants of the fetal subplate zone. It has been suggested that they perform certain important functions and may be involved in the pathogenesis of several neurological and psychiatric disorders. However, many important features of this class of human cortical neurons remain insufficiently explored. In this study, we analyzed the total number, and regional and topological distribution of WMIN in the adult human subcortical white matter, using a combined immunocytochemical (NeuN) and stereological approaches. We found that the average number of WMIN in 1 mm^3 of the subcortical white matter is 1.230 $\pm$ 549, which translates to the average total number of 593 811 183.6 $\pm$ 264 849 443.35 of WMIN in the entire subcortical telencephalic white matter. While there were no significant differences in their regional distribution, the lowest number of WMIN has been consistently observed in the limbic cortex, and the highest number in the frontal cortex. With respect to their topological distribution, the WMIN were consistently more numerous within gyral crowns, less numerous along gyral walls and least numerous at the bottom of cortical sulci (where they occupy a narrow and compact zone below the cortical-white matter border). The topological location of WMIN is also significantly correlated with their morphology: pyramidal and multipolar forms are the most numerous within gyral crowns, whereas bipolar forms predominate at the bottom of cortical sulci. Our results indicate that WMIN represent substantial neuronal population in the adult human cerebral cortex (e.g. more numerous than thalamic or basal ganglia neurons) and thus deserve more detailed morphological and functional investigations in the future.

Key words: human brain; NeuN; stereology; subplate neurons; white matter neurons.

Introduction

The cerebral white matter interstitial neurons (WMIN) are a class of neurons located within the gyral white matter, first described by Theodor Meynert in 1867 as a normal part of the human cerebral white matter (Meynert, 1867). In the following years, many studies confirmed and extended findings from the original Meynert publication (for historical details see Judaš et al. 2010a). WMIN can be found throughout the entire gyral white matter in humans as well as many experimental animals (Kostović & Rakic, 1980; Valverde & Facal-Valverde, 1988; Valverde et al. 1989; Meyer et al. 1992; Reep, 2000; Clancy et al. 2001; Okhotin & Kalinichenko, 2003; Suárez-Solá et al. 2009; García-Marín et al. 2010; Judaš et al. 2010a,b; Hoerder-Suabedissen & Molnár, 2013; Mortazavi et al. 2016; Swiegers et al. 2019). They are a diverse neuronal population expressing both glutamatergic and GABAergic markers and a wide range of morphological profiles, e.g. pyramidal, fusiform, triangular, multipolar, etc. (Kostović & Rakic, 1980; Valverde & Facal-Valverde, 1988; Valverde et al. 1989; Meyer et al. 1992; Ang & Shul, 1995; García-Marín et al. 2010; Judaš et al. 2011). Although it is difficult to study the functional role of WMIN in the human brain, many studies demonstrated their integration in the overlying cortical circuits (Shering & Lowenstein, 1994; Clancy et al. 2001; Tomioka et al. 2005; Tomioka & Rockland, 2007; Torres-Reveron & Friedlander, 2007; Von Engelhardt et al. 2011; Frazer et al. 2017). The WMIN have been associated with various functions such as vasodilation in the brain (Estrada & DeFelipe, 1998; Cauli & Hamel, 2010), sleep regulation (Kilduff et al. 2011) and information processing in the brain (Kostović et al. 2011; Colombo, 2018; Hoerder-Suabedissen et al. 2018). Furthermore, it has been suggested that WMIN have an important role in the pathology of depression (Beasley et al. 2002; Molnar et al. 2003), schizophrenia (Akbarian et al. 1996;

Correspondence
Professor Miloš Judaš, Croatian Institute for Brain Research, University of Zagreb School of Medicine, Šalata 12, 10 000 Zagreb, Croatia.
T: +385 1 4596801; E: mjudas@hiim.hr

Accepted for publication *24 April 2019*
Article published online *7 June 2019*

Anderson et al. 1996; Kirkpatrick et al. 1999, 2003; Beasley et al. 2002; Eastwood & Harrison, 2003, 2005; Molnar et al. 2003; Rioux et al. 2003; Connor et al. 2009; Fung et al. 2014; McFadden et al. 2016), bipolar disorder (Beasley et al. 2002; Connor et al. 2009), autism (Bailey et al. 1998), epilepsy (Meencke, 1983; Richter et al. 2016), Alzheimer's disease (Ang & Shul, 1995; Van de Nes et al. 2002) and multiple system atrophy (Nykjaer et al. 2017).

However, many questions about the origin, function and number of WMIN are still unresolved. Two of the most important questions about WMIN are (1) their developmental origin and (2) their total number and regional distribution in the adult brain. Initial studies on the WMIN origin suggested that they are remnant neurons of the transient fetal subplate population (Kostović & Rakic, 1980, 1990; Valverde & Facal-Valverde, 1988; Chun & Shatz, 1989a,b) and these findings were later corroborated using modern techniques (Hoerder-Suabedissen et al. 2009; Judaš et al. 2011; Hoerder-Suabedissen & Molnar, 2012; Hoerder-Suabedissen & Molnár, 2013). These studies suggested that a large portion of subplate neurons undergo apoptosis, and only a small portion of them survive to become WMIN (Luskin & Shatz, 1985; Wahle & Meyer, 1905; Valverde & Facal-Valverde, 1988; Chun & Shatz, 1989a,b; Allendoerfer & Shatz, 1994; Hoerder-Suabedissen & Molnár, 2013), although no study conclusively showed massive apoptosis in the subplate. In fact, Robertson et al. (2000) showed that the rate of apoptosis in rats in the subplate is comparable to other cortical layers. Therefore, the total number of WMIN would provide us with the solid foundation to elucidate the degree of subplate apoptosis in the human brain.

Investigations on the distribution, density and total number of WMIN are rare and often performed on primate (Mortazavi et al. 2016; Swiegers et al. 2019) rather than human (García-Marín et al. 2010) brain. Additional data about the density of WMIN can be found in neuropathological studies of the human brain (Meencke, 1983; Akbarian et al. 1996; Anderson et al. 1996; Kirkpatrick et al. 1999; Beasley et al. 2002; Eastwood & Harrison, 2003; Nykjaer et al. 2017). However, these studies are often designed to investigate pathology rather than normal distribution of WMIN. The data presented in these studies are difficult to compare due to different quantification methods, parameters and definitions of WMIN compartment. As a result, the WMIN density reported in these studies is differs widely, ranging from 1100 to 3000 WMIN per mm^3. Although the majority of studies analyzed the density of WMIN, they did not provide the data on the total number of WMIN. This piece of information would help us in assessing the functional importance of WMIN and further our understanding of its role in various brain disorders.

In the present study, we set out to investigate the distribution, density and total number of WMIN in the normal human brain. First, we defined the WMIN compartment and employed a quantitative approach on immunohistochemical slides. Furthermore, we set out to investigate whether the size and shape of gyrus and the underlying white matter influence the WMIN distribution and density. We found that WMIN represent a large neuronal population in the human brain. The WMIN distribution within gyral white matter is not uniform and it is heavily influenced by the shape of the gyrus. During the analysis of the regional distribution of WMIN, we did not observe any statistically significant differences.

Materials and methods

Tissue processing

To analyze the number of WMIN, we performed the quantification on immunocytochemistry slides of an adult human brain. In this study, we used three adult postmortem brains (postmortem delay 12–24 h) that are a part of the Zagreb Neuroembryological Collection (Kostović et al. 1991; Judaš et al. 2011). The brains were collected during routine autopsies at the Department of Pathology of the University of Zagreb School of Medicine following standard protocol approved by the Ethical Committee and the IRB of the institution and with a consent from the next of kin. Neither of the brains used in this study exhibited any macroscopical or microscopical pathology. Whole brains were immersion-fixed using 4% paraformaldehyde in 0.1 M phosphate buffer solution (pH = 7.4) for up to 1 month. Following fixation, brains were sectioned in tissue slabs of approximately 1–2 cm thickness and divided into smaller tissue blocks (Fig. 1). If signs of unsatisfactory fixation were observed after sectioning, tissue blocks were further fixed in the same fixating solution as before, for up to 48 h. After the satisfactory fixation was achieved, tissue blocks were cryoprotected using graded series of sucrose (10, 20 and 30%) and frozen. Tissue blocks were cut in a coronal plane at a thickness of 100 μm.

Immunocytochemistry and image processing

Free-floating immunocytochemistry was performed using standard protocols. Briefly, all sections were pretreated with 0.3% H_2O_2 in a 3 : 1 mixture of a methanol and distilled water in order to quench endogenous peroxidase activity, followed by a 10-min rinse in phosphate-buffered saline (PBS). To prevent nonspecific background staining, sections were immersed in the blocking solution (PBS solution containing 5% bovine serum albumin and 0.5% Triton X-100; all Sigma) for 1 h at room temperature (RT). To visualize the WMIN, sections were incubated overnight at 4 °C with a polyclonal rabbit anti-NeuN antibody (1 : 2000; Abcam, USA) reactive for the N-terminal part of the human NeuN protein. Following incubation, sections were rinsed in PBS for 1 h and then secondary biotinylated anti-rabbit antibody (Vectastain ABC kit) was applied (1 : 2000 in the blocking solution) for 1 h at RT. The sections were rinsed in PBS for 1 h and immersed in the streptavidin/peroxidase complex (1 : 500 in PBS, Vectastain ABC kit) for 1 h at RT. The peroxidase activity was visualized using Ni – 3,3-diaminobenzidine (Sigma). After visualization, sections were dehydrated in graded series of alcohol, cleared in xylene and coverslipped using Histomount (National Diagnostics, USA). In all experiments, negative controls were included either by omitting the secondary antibody or by replacing it with an anti-rabbit secondary antibody. No labeled cells were detected in these control sections. The quality of sections and qualitative analysis were

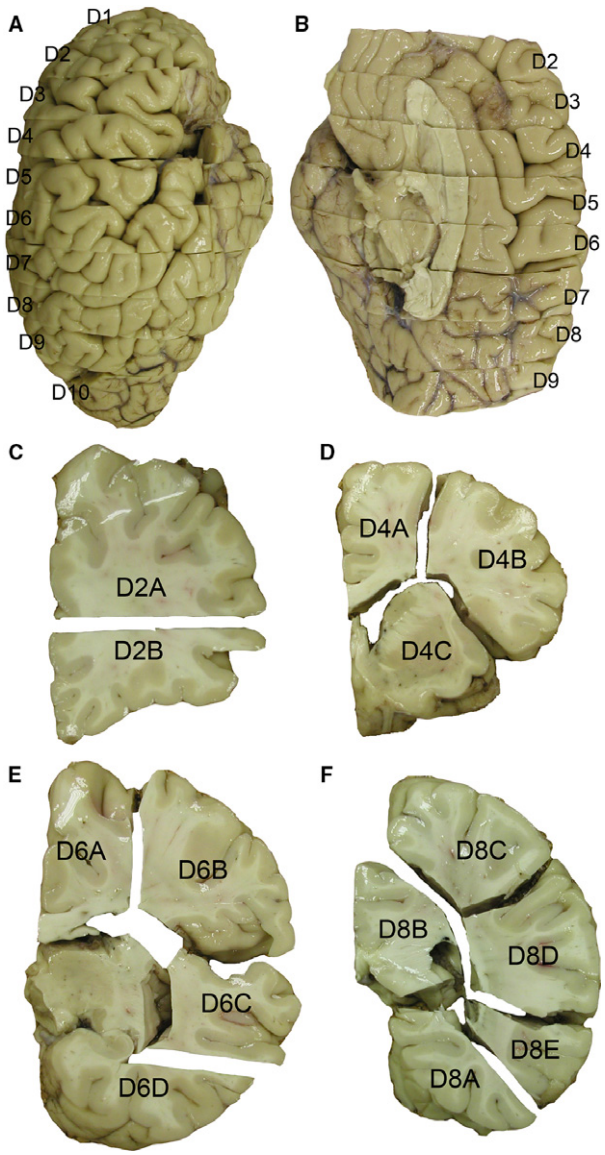

Fig. 1 Section protocol for the adult human brain. The hemisphere of the adult human brain has been cut in 10 coronal tissue slabs from the frontal to the occipital pole with thicknesses ranging from 1 to 2 cm (A,B). Each slab has been subdivided into several smaller blocks based on neuroanatomical landmarks and overall size (C–F).

done using an Olympus Provis AX70 upright microscope (Olympus). Sections were digitized using a Hamamatsu NanoZoomer 2.0 – RS digital slide scanner (Hamamatsu Photonics) at 400× magnification. Images were exported from virtual slides using NDP.VIEW2 software (Hamamatsu Photonics) and processed using Adobe PHOTOSHOP CS5 (Adobe Systems).

Quantification and distribution of white matter WMIN

NeuN immunostained sections were used to estimate the density and the distribution of WMIN in five different regions of the human brain (orbitofrontal cortex, dorsolateral prefrontal cortex, occipital cortex, temporal cortex, cingulate cortex). To be able to obtain the total number of WMIN, we analyzed the WMIN density within the von Monakow segment IV of the white matter (von Monakow), defined as the white matter up to 3 mm below cortex/white matter border (CX/WM). The upper border of this segment was determined as the border between the cerebral cortex and the white matter. Although the interface between the white matter and the cerebral cortex is relatively easy to distinguish at low magnification, this is still just an approximation as there is no clear-cut border between these two compartments. The lower border of the segment was determined by connecting two adjacent points located 3 mm within the white matter below the neighboring sulci (Fig. 2). The neuronal density was estimated by a quantification procedure adhering to stereological principles, when possible, as described in West & Gundersen (2014) using an Olympus BX51 light microscope with motorized stage (Olympus) and a Nikon DXM1200 digital camera connected to the computer equipped with a Stereo Investigator software (MBF Bioscience, USA). Counting procedures were performed on five consecutive sections (100 μm thick) in all regions analyzed. Optical dissectors were obtained using a 60× objective. The total counting surface was 10 577,40 mm^2. A neuron was counted only if a clearly identifiable cell body could be visualized at the height of the optical plane along the *z* axis. The total number of counted neurons was 10 123. All statistical analyses were done using a GraphPad PRISM 6 (GraphPad Software, USA). All reported values are given as mean ± standard deviation.

Magnetic resonance (MR) imaging white matter volume

To determine the volume of the von Monakow segment IV, MR imaging of four healthy volunteers was done. Images were recorded using a 12-channel head-coil, with a 3D MPRAGE sequence in a sagittal plane with the following parameters: TR/TE = 2300/3 ms; inflection angle = 9°, matrix = 256 × 256, voxel size = 1 × 1 × 1 mm. The volumetric analysis was done using an automatic segmentation method using the CIVET software (McGill University, Montreal, Canada), which automatically defines the border between different brain volumes (gray matter, white matter, cerebrospinal fluid) based on the difference in the voxel intensity. After delineating the white matter from the rest of the brain, the volume of the von Monakow segment IV was determined using the ANALYZE 8.1 software (Mayo Clinic, USA). The lower border of the segment was determined in the same way as described for histological slides. The volume of the determined von Monakow segment IV white matter was used to estimate the total number of WMIN in the human brain.

Results

Visualization, localization and distribution of WMIN

We used the NeuN antibody to visualize WMIN in our histological preparation. NeuN staining has allowed us to recognize only the neurons within the white matter; this is especially important for smaller neurons, which sometimes can be mistaken for glial cells and *vice versa* in Nissl slides. The majority of WMIN are located close to the CX/WM border, which significantly complicates any cell-counting studies (Fig. 3). The density of WMIN decreases from the CX/

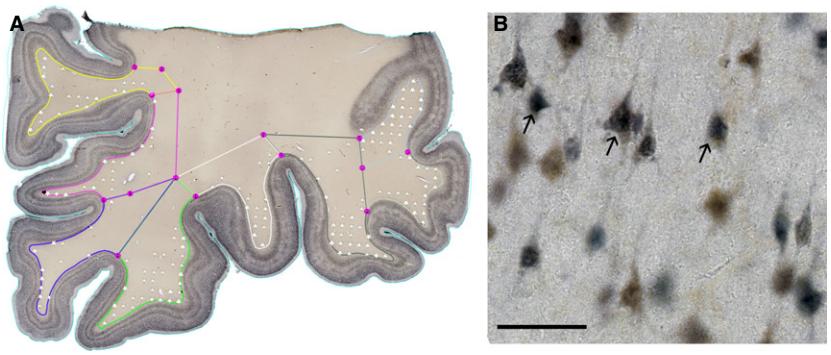

Fig. 2 Representative NeuN histological section with overlying counting grid. The figure depicts borders of the von Monakow segment IV (different colors) on the actual histological slide (A). White stars in (A) depict counting sites where WMIN neurons were recorded. (B) Higher magnification of NeuN-positive slides with WMIN. Arrows point to the examples of cells considered positive for counting procedures. Scale bar: 50 μm.

WM border towards the center of the gyral white matter. However, the decrease is not uniform throughout the entire gyrus. In the crown of gyri, WMIN are more dispersed and the drop in density is less pronounced moving farther away from CX/WM border (Fig. 3). On the other hand, under the sulci the WMIN are more compact and located closer to the CX/WM border; thus the drop in density is steeper moving farther away from CX/WM border. The described pattern of WMIN distribution within the gyri was observed in all analyzed types of gyri and in all analyzed regions.

Regional density and the total number of WMIN

To determine whether there are regional differences in the density of WMIN, we analyzed five regions of the cerebral cortex: orbitofrontal, limbic, dorsolateral prefrontal, temporal and occipital cortex (Table 1). The lowest density of WMIN was observed in the cingulate cortex (1010 $\pm$ 344.1 neurons per mm^3), followed by the orbitofrontal cortex (1057 $\pm$ 387.2 neurons per mm^3). The highest density of WMIN was observed in the dorsolateral prefrontal cortex (1331 $\pm$ 533 neurons per mm^3). There were no statistically significant differences between the analyzed regions, except the orbitofrontal and the dorsolateral prefrontal cortex.

Due to the specific spatial distribution of WMIN within the gyrus, we investigated whether there are any observable differences between different types of gyri (Fig. 4). In general, smaller gyri with a smaller area of white matter tend to have a greater density of WMIN than larger gyri do (Fig. 5). However, larger gyri have a greater estimated total number of WMIN.

To estimate the total number of WMIN in the human brain, we measured the total volume of von Monakow segment IV on MR images of healthy adult brains. The measured volume of segment IV was 482 773,32 mm^3. The mean density of WMIN in all regions in all analyzed brains was 1230 $\pm$ 548.6 neurons per mm^3. Estimated total number of WMIN in the entire human white matter was 593 811 183,6 $\pm$ 264 849 443,35 neurons.

Discussion

In the present study we provided data on distribution, density and total number of WMIN. As previously reported, WMIN are not uniformly distributed throughout the gyral white matter (Meyer et al. 1992; Akbarian et al. 1996; Beasley et al. 2002; García-Marín et al. 2010; Mortazavi et al. 2016; Swiegers et al. 2019). We expanded these findings by providing evidence that size and shape of the gyral white matter have a significant influence on the distribution of WMIN. In general, smaller, narrower gyri will have a greater density of WMIN and larger, wider gyri will have a smaller density, although they will have a larger total number or WMIN. Therefore, when analyzing the distribution and density of WMIN one must also bear in mind the gyral architecture. Our data indicate that WMIN are a substantial population of neurons located in the gyral white matter of the human brain. Although in this study we provide estimates that WMIN are a large population, our study, as well as all others dealing with WMIN quantification suffer from some technical limitations. There are several important features that one must be aware of when quantifying WMIN or comparing the data presented in various studies.

Quantification procedure and the definition of WMIN compartment

Today, the gold standard for determining neuronal number or density in three-dimensional, microscopic structure is stereology. However, many prerequisites need to be fulfilled for stereology to provide confident, replicable data. One of the prerequisites is precise delineation of the investigated structure, in order to sample the whole structure in an unbiased manner (Gundersen & Osterby, 1981; West &

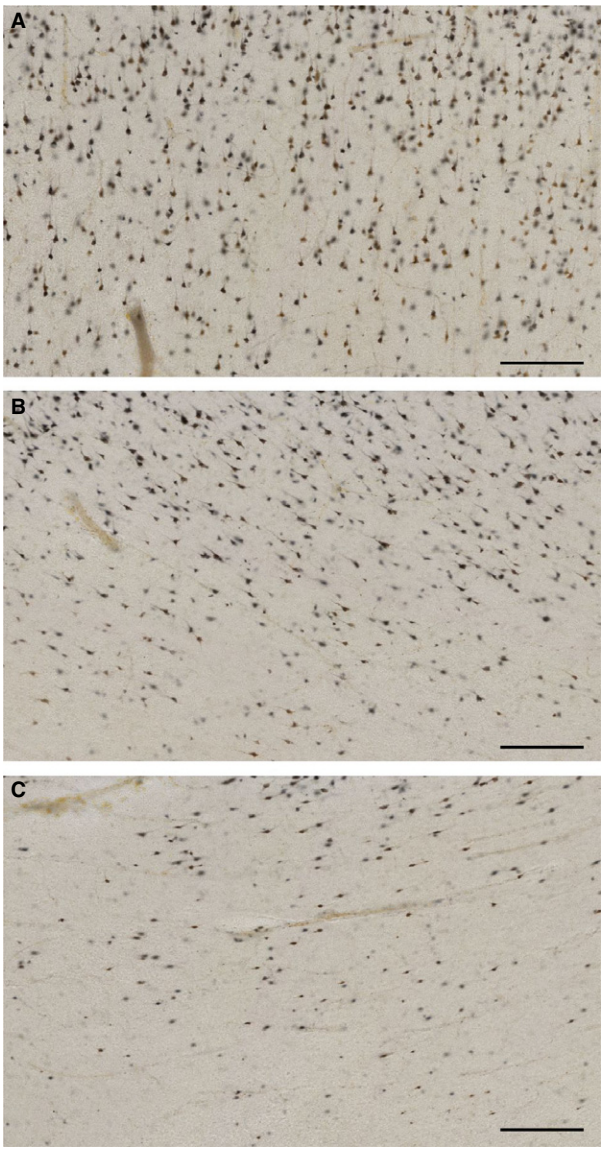

Fig. 3 White matter interstitial neuron density within the gyrus and sulcus. NeuN images depicting the differences in WMIN densities in the crown of the gyrus (A), gyral wall (B) and at the bottom of the sulcus (C). Please note that the density of WMIN gradually reduces from the gyral crown to the bottom of the sulcus. Scale bar: 200 μm.

Gundersen, 2014; Boyce et al. 2010). This prerequisite often cannot be completed when analyzing the cerebral cortex and is even more difficult when analyzing WMIN in highly gyrencephalic brain. The first problem with this prerequisite is that for WMIN we do not know what is 'the entire structure'. There are not enough data about the regional differences, or a map similar to Brodmann's map, to delineate individual regions or areas (as one can do with cortical areas; Mortazavi et al. 2016). Furthermore, in the gyrencephalic brain, it is sometimes possible to cut tangentially through WMIN without even realizing it (e.g. when gyrus is so convoluted that one part of it gets 'stuck' very deep in the white matter; Fig. 6). Therefore, it is often necessary to 'select' specific histological slides for quantification, which precludes the unbiased prerequisite. The human brain is an inherently anisotropic structure, already a significant problem for stereology (and thus for the necessity of unbiased sampling and counting). WMIN are even more anisotropic, as the majority of WMIN are located close to the CX/WM border. Therefore, one must 'adjust' the sampling protocol to favor the superficial parts of the sample in order not to underestimate the number of WMIN. In our sample, we deliberately selected certain parts of the white matter to cover as wide as possible range of different types of gyri and to avoid possible 'overrepresentation' of WMIN due to the tangential cuts.

Table 1 Regional density of WMIN neurons

AREA	WMIN density per mm^3	CV
Orbitofrontal cortex	1057 ± 387.2	0.37
Cingulate cortex	1010 ± 344.1	0.34
Dorsolateral cortex	1331 ± 533.0	0.4
Temporal cortex	1115 ± 372.0	0.33
Occipital cortex	1208 ± 505.0	0.42

An additional problem in WMIN quantifying is the determination of WMIN compartment borders. Many authors have recognized the difficulty of reliably defining the CX/WM border (García-Marín et al. 2010; Mortazavi et al. 2016; Swiegers et al. 2019). Although at lower magnifications the CX/WM border is easier to recognize, the placement of the border is still not very reliable. The determination of the border is based on the individual preferences of each investigator, even when in principle the exact set of parameters for defining borders has been used (Fig. 6). As the largest number of WMIN are located close to the border of CX/WM, the differences in placing CX/WM border could significantly influence the density and total number of WMIN. Without the specific marker of WMIN it will be difficult to determine the upper border of the WMIN compartment reliably.

Similarly, to the upper border of the WMIN compartment, the precise lower border of the compartment has not been consistently defined. In fact, the main difference between studies dealing with WMIN density is the definition of counting area and consequently WMIN compartment. Usually the selected counting area has been defined either as a surface with arbitrary thickness from the CX/WM border or a counting frame of preselected size placed beneath the CX/WM border. As a result, the counting area that is closer to the CX/WM border will yield a greater density of WMIN, whereas counting areas further away from the CX/WM border will produce a lower density of WMIN (for example see García-Marín et al. 2010 superficial and deep compartment). We

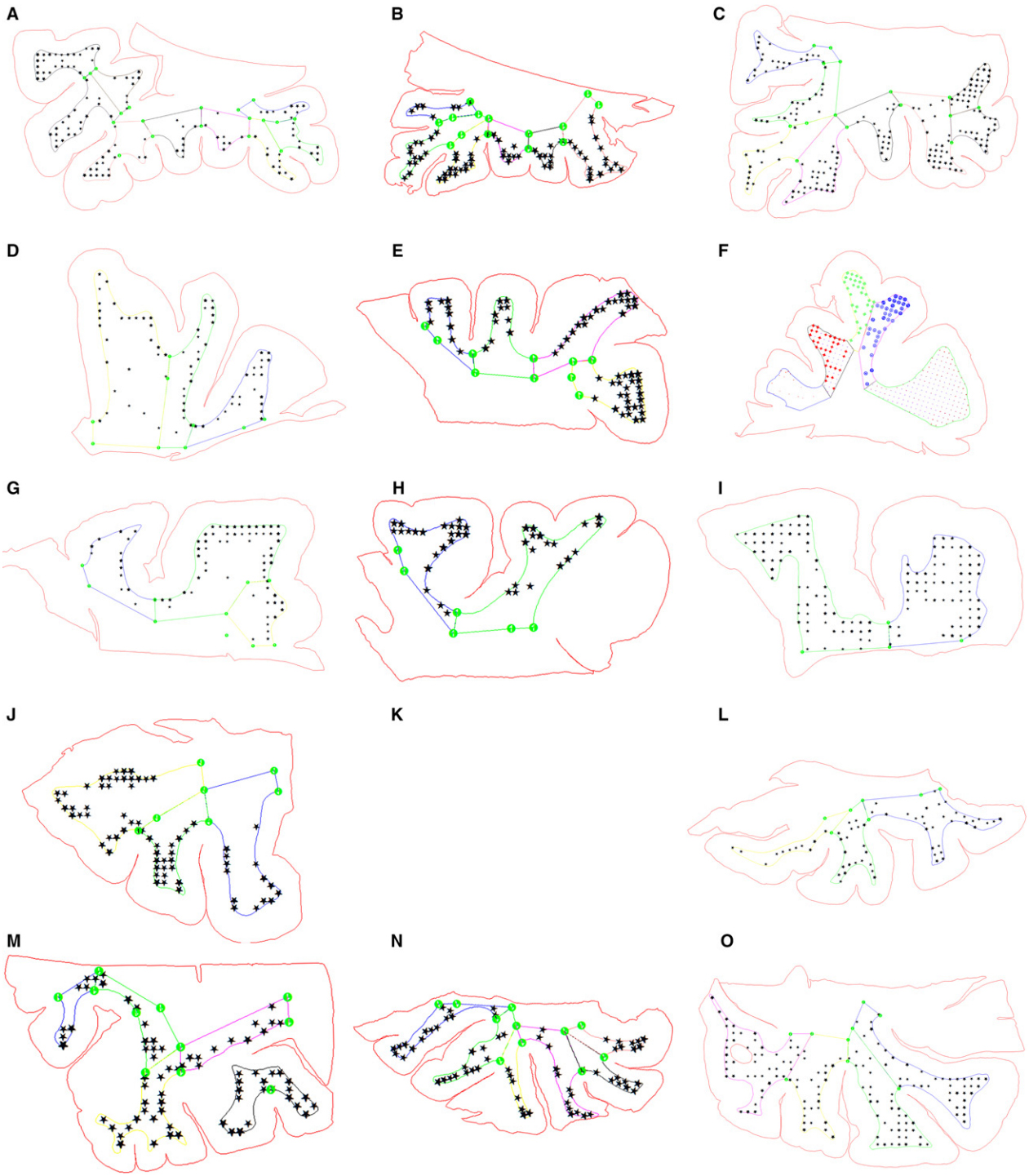

Fig. 4 Representation of counting sites in different brains and different regions. The red line depicts the contour of the section and the color lines depict the borders of the von Monakow segment IV. Black dots represent the counting sites in different brain areas. Orbitofrontal cortex (A–C), Medial and dorsolateral prefrontal cortex (D–I), Medial and inferior temporal cortex (J, K) and occipital cortex (L–N).

believe that to provide more reliable and reproducible data, a WMIN compartment must be defined based on the neurodevelopmental data.

In our study, we selected the von Monakow segment IV of the white matter as the WMIN compartment. We defined this compartment as an area of white matter adjacent to the cerebral cortex and up to 3 mm of white matter beneath cortex. We chose this compartment and definition based on the neurodevelopmental data about the origin of WMIN. In many studies it has been demonstrated that

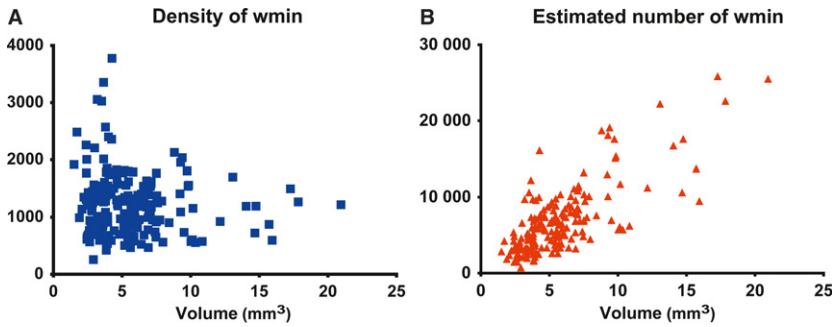

Fig. 5 WMIN density and estimated number of neurons based on the size of the gyral white matter. Note that gyri with the largest WMIN density have a smaller volume of white matter (A), although gyri with the largest estimate of the WMIN have a large white matter volume (B).

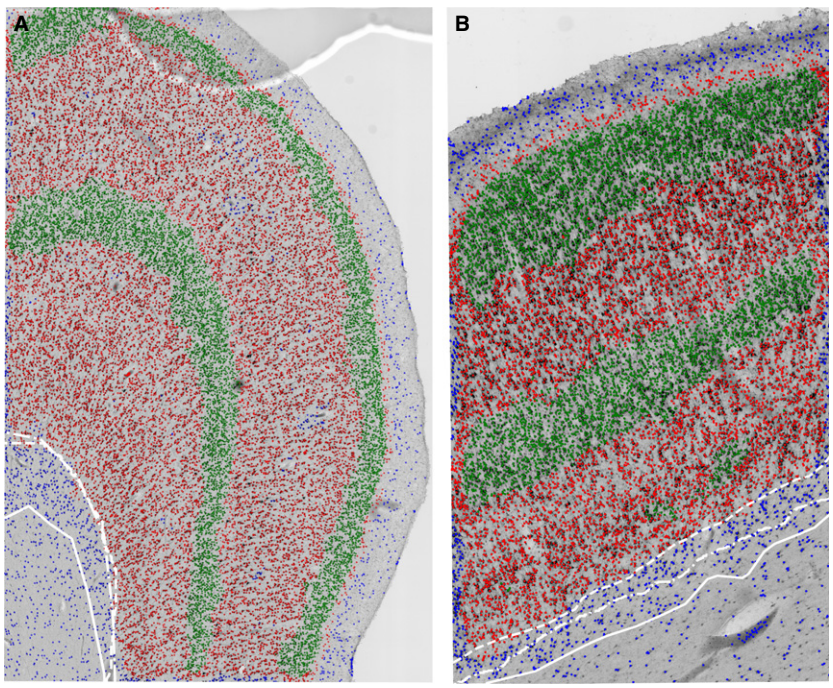

Fig. 6 The differences of CX/WM border placement between different investigators and computer algorithm. The main feature used to distinguish CX from WM was a sharp drop in neuronal density. Please note that when three experienced investigators used this feature to place the CX/WM border, a significant difference could be observed (white lines in A,B), especially in regions where WMIN are denser under the border (B). Use of an automatic algorithm would perform this task in the same manner every time, ensuring the reproducibility of data. Neurons are classified based on the density: blue dots – very rare, green dots – very dense, red dots – intermediate.

WMIN are remnants of subplate neurons (Kostović & Rakic, 1980, 1990; Valverde & Facal-Valverde, 1988; Chun & Shatz, 1989a,b; Hoerder-Suabedissen et al. 2009; Judaš et al. 2011; Kostović et al. 2011; Hoerder-Suabedissen & Molnar, 2012, 2013; Frazer et al. 2017). During development, the subplate zone is the largest transient zone of the human telencephalic wall, reaching up to 5 mm below the cortical plate (Kostović & Rakic, 1990). Following the dissolution of the subplate zone, this area is invaded at the bottom part by long cortico-cortical and cortico-subcortical white matter fibers and at the top by short cortico-cortical (gyral) white matter fibers (Kostović et al. 2014a,b; Žunić Išasegi et al. 1990). The selected thickness of 3 mm is well within the maximal size of the subplate zone during development (Kostović & Rakic, 1990), which gives us confidence that neurons located in this compartment are truly remnants of subplate neurons – WMIN. By defining the WMIN compartment in such a way, we are proposing the solution to one of the major problems for any study trying to elucidate the number or density of WMIN. Our and previous studies have shown that the density of WMIN is larger closer to the CX/WM border. By selecting different counting areas in different studies, one can artificially increase or decrease the density and number of WMIN by overestimating or

underestimating the surface in which neurons reside. This is also the main reason for the discrepancy between studies when reporting WMIN density in various regions. As we demonstrated, the distribution of WMIN and consequently the density of WMIN greatly depend on the local architecture of the white matter. By defining smaller counting areas, combined with the uncertainty of CX/WM border, one can unintentionally introduce the differences between the brain regions as artifacts of sampling procedure. Our proposition to define the WMIN compartment based on neurodevelopmental data would greatly reduce, although not remove completely, the potential for this kind of error to impact the results.

Only a handful of studies investigated WMIN density using pan-neuronal markers, with densities ranging from 1100 to 3000 WMIN per mm^3 (Meencke, 1983; Eastwood & Harrison, 2005; García-Marín et al. 2010; Richter et al. 2016). In our dataset the mean density of WMIN was 1145 ± 428.26 neurons mm^{-3}. Direct comparison of our results with other studies is not possible due to the aforementioned reasons. Each study used a different size of counting compartment, from predetermined counting box (Eastwood & Harrison, 2005) to entire white matter in analyzed section (Richter et al. 2016), thus yielding different WMIN densities. A study that is the most comparable to ours is from García-Marín et al. (2010). Like our study, they analyzed WMIN density in five brain regions. However, they divided gyral white matter into two compartments (superficial and deep), with an approximate thickness of 175 μm. In that study they found that there are regional differences in WMIN density and that the greatest WMIN density is in the frontal cortex, followed by the cingulate cortex, and the lowest density was observed in the temporal cortex. The observed difference was only present in the superficial compartment and not in the deep one. In contrast, in our dataset we did not observe statistically significant differences between the cortical regions. Furthermore, we observed the greatest density of WMIN in the dorsolateral prefrontal cortex although in our sample the lowest density is in the cingulate cortex. García-Marín et al. (2010) also reported the higher mean density of WMIN than we observed in our sample. The observed differences in WMIN density between two studies could be explained by the smaller counting compartment in the study of García-Marín et al. Their counting compartment was rather 'thin', measuring only 350 μm, whereas our WMIN compartment spanned up to 3 mm in depth. Furthermore, their superficial compartment was located close to the CX/WM border which, due to the intrinsic arrangement of WMIN, would yield a higher density of WMIN. Both studies observed high interindividual variability between samples.

The only study that used a counting compartment similar to ours was by Meencke (1983). In that study the entire white matter of a single gyrus was used as a counting compartment. Interestingly, when the data presented in that study are transformed to our unit of measurement (WMIN mm^{-3} instead of the reported 0.005 mm^{-3}), a very similar WMIN density is observed in both studies. Meencke reported a density of 1140 neurons mm^{-3}, which is similar to our 1230 ± 548.6 neurons mm^{-3}. This result indicates that if a similar WMIN compartment is used for quantification, the reported densities would be more consistent.

Based on our data, we estimated that there are more than half a billion WMIN in the human brain. To our knowledge, the only other study reporting the total number of WMIN was from Nykjaer et al. (2017). That study was designed as an unbiased stereological quantification set to investigate the loss of cells in the white matter in patients with multiple system atrophy. Nykjaer et al. concluded that there are around 1.1 billion WMIN in the human brain. Their estimate is almost twice the size of our estimate of the total number of WMIN. In this study, the authors applied stereology to assess WMIN, which included unbiased, random sectioning of the entire human brain hemisphere. As we mentioned above, if the architecture of the white matter is not considered, one could overestimate or underestimate the number of WMIN. Furthermore, the authors observed large interindividual differences between the analyzed samples, as we did in our samples. The discrepancies between our findings could be explained by different sampling methods and interindividual differences. However, both studies found that WMIN are a large neuronal population in the human brain. Additional studies designed to accommodate the above-mentioned problems when quantifying WMIN.

WMIN, a large yet under-appreciated neuronal population

Our data and data from other studies indicate that WMIN are a substantial neuronal population in the human brain. The average total number of WMIN in the adult human brain is in the range of 450–670 million neurons. To appreciate how extensive and important this population of neurons is, it is useful to compare it with the total number of neurons in the entire brain or the entire cerebral cortex of various mammalian species, as recently summarized in the work of Susana Herculano-Houzel (Herculano-Houzel, 2016; pp. 217–226). WMIN represent approximately 3.5% of all neurons in the human cerebral cortex, but their population is as large as 8 mouse brains, 3 rat brains, 1 rabbit brain or 1 marmoset brain, or 40× larger than the cerebral cortex of mouse, 18× larger than the cortex of rat, 8× larger than the cortex of rabbit, 2× larger than the cortex of marmoset or cortex of pig. On the other hand, the human WMIN neuron population is as large as the one-third of the entire owl monkey cortex, or half of the capuchin or squirrel monkey cerebral cortexes. Furthermore, when compared with other functionally important brain structures, WMIN are a significantly

larger population. Recently, Wegiel et al. (1987) reported the total number of neurons in basal ganglia and other important structures (such as hippocampal formation or cerebellum) in the human brain. By comparing the number of WMIN with the results, we can see that WMIN population is as big as 8 putamen, 10 caudate nuclei, 10 thalami, 40 claustrum nuclei, 50 amygdalae and 400 globus pallidi neuronal populations (Wegiel et al. 1987). If you compare it to some cortical structures, WMIN are 40× larger than the entorhinal cortex and 30× larger than the population of Purkinje cells (Wegiel et al. 1987). Although, WMIN are more numerous than some cortical structures, the density of WMIN is nonetheless significantly lower. For example, the average neuronal density is approximately 47 000 neurons mm^{-3} in the prefrontal cortex, making it 35× denser than WMIN in the same region (Thune et al. 2001), and approximately 45 000 neurons mm^{-3} in the orbitofrontal cortex, making it 40× denser than WMIN (De Oliveira et al. 2019).

Such a large population must have a significant role in the normal functioning of the cerebral cortex. At the moment, it is impossible to investigate directly the functional role of WMIN in the human brain. It is only possible to make speculations based on indirect evidence about the importance of this neuronal population. Some investigators already proposed the role of WMIN in blood flow regulation, sleep regulation and information processing in the brain. We believe that WMIN are positioned at the key place in the white matter to regulate the information flow between adjacent cortical regions. As we previously argued (see Kostović et al. 2011), we believe that WMIN are 'gatekeepers' and 'integrators' of cortical circuits. During the development of the cerebral cortex, subplate neurons have a key function of transferring and regulating the information flow between the cortex and subcortical structures. As the WMIN neurons are remnants of the subplate zone, we propose that they retain these abilities. However, their main partners in the adult brain are not subcortical neurons but rather short, cortico-cortically projecting neurons. The development of short cortico-cortical fibers is a late event (after the 30th postconceptional week') coinciding with the resolution of the subplate zone. When subcortical afferents migrate away from subplate neurons to the cortical plate, subplate neurons must maintain connectivity in order to survive. We propose that short cortico-cortical fibers fill this gap and form a permanent link, which is maintained in the adulthood. If our theory is correct, this would provide a possible explanation for the involvement of WMIN in many brain disorders and the key position of WMIN in the regulation of the information flow in the cerebral cortex.

Future directions

In the present study, we demonstrated that WMIN are a substantial population of neurons in the human white matter. However, the methodology used in this study has certain limitations, as discussed above. To quantify WMIN more precisely, a more reliable way of determining the WMIN population should be developed. One possible avenue is to elucidate the molecular markers specific for this neuronal population. This would make it easier to determine the WMIN population and the size of the compartment, which is important for determining the neuronal density and consequentially the total neuronal number. Although several groups are already working on elucidating the molecular profile of the subplate and WMIN neurons (Hoerder-Suabedissen & Molnár, 2013, 2013; Pedraza et al. 2014; Frazer et al. 2017; Viswanathan et al. 2017), there is still no marker available that would encompass the entire population. Another approach is to better differentiate the border between CX and WM. When delineating cortical layers, human investigators are inherently biased by their experience, education or preferences. Therefore, we are currently developing a computer algorithm which could reliably and reproducibly recognize neurons and the cortical layer. Initial studies have shown that it is possible automatically to delineate the border between the cerebral cortex and white matter (Fig. 6) with great reproducibility and a high degree of confidence. When employing an automated procedure, we consistently label the same population of neurons, allowing us to remove the majority of errors plaguing WMIN quantification (the differences in the CX/WM border, the size of counting area, the definition of the population, etc.). Furthermore, this algorithm is capable of quantifying all labeled neurons, thus removing the need to estimate the total number of neurons. If either of these approaches bears any results, the investigation of WMIN will be greatly advanced.

Acknowledgements

This work was supported by the Unity Through Knowledge Fund grant no. 9/17 (G.S.) and co-financed by the European Union through the European Regional Development Fund, Operational Program Competitiveness and Cohesion, grant agreement No. KK.01.1.1.01.0007, CoRE - Neuro. (M.J). G.S. performed all of the experiments. G.S. and M.J. designed the study, analyzed the data and wrote the manuscript. We thank Andrija Štajduhar for providing us with the data about the automatic cell recognition algorithm.

References

Akbarian S, Kim JJ, Potkin SG, et al. (1996) Maldistribution of interstitial neurons in prefrontal white matter of the brains of schizophrenic patients. *Arch Gen Psychiatry* **53**, 425–436.

Allendoerfer KL, Shatz CJ (1994) The subplate, a transient neocortical structure: its role in the development of connections between thalamus and cortex. *Annu Rev Neurosci* **17**, 185–218.

Anderson SA, Volk DW, Lewis DA (1996) Increased density of microtubule associated protein 2-immunoreactive neurons in

the prefrontal white matter of schizophrenic subjects. *Schizophr Res* **19**, 111–119.

Ang LC, Shul DD (1995) Peptidergic neurons of subcortical white matter in aging and Alzheimer's brain. *Brain Res* **674**, 329–335.

Bailey A, Luthert P, Dean A, et al. (1998) A clinicopathological study of autism. *Brain* **121**, 889–905.

Beasley CL, Cotter DR, Everall P (2002) Density and distribution of white matter neurons in schizophrenia, bipolar disorder and major depressive disorder: no evidence for abnormalities of neuronal migration. *Mol Psychiatry* **7**, 564–570.

Boyce JT, Dorph-Petersen KA, Lyck L, et al. (2010) Design-based stereology: introduction to basic concepts and practical approaches for estimation of cell numbers. *Toxicol Pathol* **38**, 1011–1025.

Cauli B, Hamel E (2010) Revisiting the role of neurons in neurovascular coupling. *Front Neuroenergetics* **2**, 9.

Chun JJM, Shatz CJ (1989a) Interstitial cells of the adult neocortical white matter are the remnant of the early generated subplate neuron population. *J Comp Neurol* **282**, 555–569.

Chun JJM, Shatz CJ (1989b) The earliest-generated neurons of the cat cerebral cortex: characterization by MAP2 and neurotransmitter immunohistochemistry during fetal life. *J Neurosci* **9**, 1648–1667.

Clancy B, Silva-Filho M, Friedlander MJ (2001) Structure and projections of white matter neurons in the postnatal rat visual cortex. *J Comp Neurol* **434**, 233–252.

Colombo JA (2018) Cellular complexity in subcortical white matter: a distributed control circuit? *Brain Struct Funct* **223**, 981–985.

Connor CM, Guo Y, Akbarian S (2009) Cingulate white matter neurons in schizoprenia and bipolar disorder. *Biol Psychiatry* **66**, 486–493.

De Oliveira KC, Grinberg LT, Hoxter MQ, et al. (2019) Layer-specific reduced neuronal density in the orbitofrontal cortex of older adults with obsessive-compulsive disorder. *Brain Struct Funct* **224**, 191–203.

Eastwood SL, Harrison PJ (2003) Interstitial white matter neurons express less reelin and are abnormally distributed in schizophrenia: towards an integration of molecular and morphologic aspects of the neurodevelopmental hypothesis. *Mol Psychiatry* **8**, 821–831.

Eastwood SL, Harrison PJ (2005) Interstitial white matter neuron density in the dorsolateral prefrontal cortex and parahippocampal gyrus in schizophrenia. *Schizophr Res* **79**, 181–188.

Estrada C, DeFelipe J (1998) Nitric oxide-producing neurons in the neocortex: morphological and functional relationship with intraparenchymal microvasculature. *Cereb Cortex* **8**, 193–203.

Frazer S, Prados J, Niquille M, et al. (2017) Transcriptomic and anatomic parcellation of 5-HT_{3A}R expressing cortical interneuron subtypes revealed by single-cell RNA sequencing. *Nat Commun* **8**, 14219.

Fung SJ, Joshi D, Fillman SG, Weickert CS (2014) High white matter neuron density with elevated cortical cytokine expression in Schizophrenia. *Biol Pshychiatry* **75**, e5–e7.

García-Marín V, Blazquez-Llorca L, Rodriguez JR, et al. (2010) Differential distribution of neurons in the gyral white matter of the human cerebral cortex. *J Comp Neurol* **518**, 4740–4759.

Gundersen HJ, Osterby R (1981) Optimizing sampling efficiency of stereological studies in biology: or 'do more less well!'. *J Microsc* **121**, 65–73.

Herculano-Houzel S (2016) *The Human Advantage. A New Understanding of How Our Brain Became Remarkable*, pp. 217–226. Cambridge: The MIT Press

Hoerder-Suabedissen A, Molnar Z (2012) Morphology of mouse subplate cells with identified projection targets changes with age. *J Comp Neurol* **520**, 174–185.

Hoerder-Suabedissen A, Molnár Z (2013) Molecular diversity of early-born subplate neurons. *Cereb Cortex* **23**, 1473–1483.

Hoerder-Suabedissen A, Wang WZ, Lee S, et al. (2009) Novel markers reveal subpopulations of subplate neurons in the murine cerebral cortex. *Cereb Cortex* **19**, 1738–1750.

Hoerder-Suabedissen A, Hayashi S, Upton L, et al. (2018) Subset of cortical layer 6b neurons selectively innervates higher order thalamic nuclei in mice. *Cereb Cortex* **28**, 1882–1897.

Judaš M, Sedmak G, Pletikos M (2010a) Early history of subplate and interstitial neurons: form Theodor Meynert (1867) to the discovery of the subplate zone (1974). *J Anat* **217**, 344–367.

Judaš M, Sedmak G, Pletikos M, et al. (2010b) Population of subplate and interstitial neurons in fetal and adult human telencephalon. *J Anat* **217**, 381–399.

Judaš M, Šimić G, Petanjek Z, et al. (2011) The Zagreb collection of human brains: a unique, versatile, but underexploited resource for the neuroscience community. *Ann N Y Acad Sci* **1225**(Suppl 1), E105–E130.

Kilduff TS, Cauli B, Gerashchenko D (2011) Activation of cortical interneurons during sleep: an anatomical link to homeostatic sleep regulation. *Trends Neurosci* **34**, 10–19.

Kirkpatrick B, Conley RC, Kakoyannis A, et al. (1999) Interstitial cells of the white matter in the inferior parietal cortex in schizophrenia: an unbiased cell-counting study. *Synapse* **34**, 95–102.

Kirkpatrick B, Messias NC, Conley RR, et al. (2003) Interstitial cells of the white matter in the dorsolateral prefrontal cortex in deficit and nondeficit schizophrenia. *J Nerv Ment Dis* **191**, 563–567.

Kostović I, Rakic P (1980) Cytology and time of origin of interstitial neurons in the white matter in infant and adult human and monkey telencephalon. *J Neurocytol* **9**, 219–242.

Kostović I, Rakic P (1990) Developmental history of the transient subplate zone in the visual and somatosensory cortex of the macaque monkey and human brain. *J Comp Neurol* **297**, 441–470.

Kostović I, Judaš M, Kostović-Knežević L, et al. (1991) Zagreb research collection of human brains for developmental neurobiologists and clinical neuroscientists. *Int J Dev Biol* **35**, 215–230.

Kostović I, Judaš M, Sedmak G (2011) Developmental history of the subplate zone, subplate neurons and interstitial white matter neurons: relevance for schizophrenia. *Int J Dev Neurosci* **29**, 193–205.

Kostović I, Jovanov-Milošević N, Radoš M, et al. (2014a) Perinatal and early postnatal reorganization of the subplate and related cellular compartments in the human cerebral wall as revealed by histological and MRI approaches. *Brain Struct Funct* **219**, 231–253.

Kostović I, Kostović-Srzentić M, Benjak V, et al. (2014b) Developmental dynamics of radial vulnerability in the cerebral compartments in preterm infants and neonates. *Front Neurol* **5**, 139.

Luskin MB, Shatz CJ (1985) Studies of the earliest generated cells of the cat's visual cortex: cogeneration of subplate and marginal zones. *J Neurosci* **5**, 1062–1076.

McFadden WC, Jaffe AE, Ye T, Paltan-Ortiz JD, Hyde TM, Kleinman JE (2016) Assessment of genetic risk for distribution of total interstitial white matter neurons in dorsolateral

prefrontal cortex: role in schizophrenia. *Schiziphr Res* **176**, 141–143.

Meencke HJ (1983) The density of dystopic neurons in the white matter of the gyrus frontalis inferior in epilepsies. *J Neurol* **230**, 171–181.

Meyer G, Wahle P, Castaneyra-Perdomo A, et al. (1992) Morphology of neurons in the white matter of the adult human neocortex. *Exp Brain Res* **88**, 204–212.

Meynert T (1867) Der Bau der Grosshirnrinde und seine örtlichen Verschiedenheiten, nebst einem pathologisch-anatomischen Corollarium. *Vierteljahresschr Psychiatrie* **1**, 77–93, 126-170, 198-217.

Molnar M, Potkin SG, Bunney WE, et al. (2003) mRNA expression patterns and distribution of white matter neurons in dorsolateral prefrontal cortex of depressed patients differ from those in schizophrenia patients. *Biol Psychiatry* **53**, 39–47.

Mortazavi F, Wang X, Rosene DL, et al. (2016) White matter neuros in young adult and aged rhesus monkey. *Front Neuroanat* **10**, 15.

Nykjaer CH, Brudek T, Salvesen L, et al. (2017) Changes in the cell population in brain white matter in multiple system atrophy. *Mov Disord* **32**, 1074–1082.

Okhotin VE, Kalinichenko SG (2003) Subcortical white matter interstitial neurons: their connections, neurochemical specialization, and role in the histogenesis of the cortex. *Neurosci Behav Physiol* **33**, 177–194.

Pedraza M, Hoerder-Suabedissen A, Albert-Maestro MA, et al. (2014) Extracortical origin of some murine subplate cell populations. *Proc Natl Acad Sci U S A* **111**, 8613–8618.

Reep RL (2000) Cortical layer VII and persistent subplate cells in mammalian brains. *Brain Behav Evol* **56**, 212–234.

Richter Z, Janszky J, Setalo G Jr, et al. (2016) Characterization of neurons in the cortical white matter in human temporal lobe epilepsy. *Neuroscience* **333**, 140–150.

Rioux L, Nissanov J, Lauber K, et al. (2003) Distribution of microtubule-associated protein MAP2-immunoreactive interstitial neurons in the parahippocampal white matter in subjects with schizophrenia. *Am J Psychiatry* **160**, 149–155.

Robertson RT, Annis CM, Baratta J, et al. (2000) Do subplate neurons comprise a transient population of cells in developing neocortex of rats? *J Comp Neurol* **426**, 632–650.

Shering AF, Lowenstein PR (1994) Neocortex provides direct synaptic input to interstititat neurons of the intermediate zone of kittens and white matter of cats: a light and electron microscopic study. *J Comp Neurol* **347**, 433–443.

Suárez-Solá ML, González-Delgado FJ, Pueyo-Morlans M, et al. (2009) Neurons in the white matter of the adult human neocortex. *Front Neuroanat* **3**, 7.

Swiegers J, Bhagwandin A, Sherwood CC, et al. (2019) The distribution, number and certain neurochemical identities of infracortical white matter neurons in a lar gibbon (*Hylobates lar*) brain. *J Comp Neurol* 527, 1633–1653.

Thune JJ, Uylings HBM, Pakkenberg B (2001) No deficit in total number of neurons in the prefrontal cortex of schizophrenics. *J Psych Res* **35**, 15–21.

Tomioka R, Rockland KS (2007) Long-distance corticocortical GABAergic neurons in the adult monkey white and gray matter. *J Comp Neurol* **505**, 526–538.

Tomioka R, Okamoto K, Furuta T, et al. (2005) Demonstration of long-range GABAergic connections distributed throughout the mouse neocortex. *Eur J Neurosci* **21**, 1587–1600.

Torres-Reveron J, Friedlander MJ (2007) Properties of persistent postnatal cortical subplate neurons. *J Neurosci* **27**, 9962–9974.

Valverde F, Facal-Valverde MV (1988) Postnatal development of interstitial (subplate) cells in the white matter of the temporal cortex of kittens: a correlated Golgi and electron microscopic study. *J Comp Neurol* **269**, 168–192.

Valverde F, Facal-Valverde MV, Santacana M, et al. (1989) Development and differentiation of early generated cells of sublayer VIb in the somatosensory cortex of the rat: a correlated Golgi and autoradiographic study. *J Comp Neurol* **290**, 118–140.

Van de Nes JAP, Sandmann-Keil D, Braak H (2002) Interstitial cells subjacent to the entorhinal region expressing somatostatin-28 immunoreactivity are susceptible to development of Alzheimer's disease related cytoskeletal changes. *Acta Neuropathol* **104**, 351–356.

Viswanathan S, Sheikh A, Looger LL, et al. (2017) Molecularly defined subplate neurons project both to thalamocortical recipient layers and thalamus. *Cereb Cortex* **27**, 4759–4768.

Von Engelhardt J, Khrulev S, Eliava M, et al. (2011) 5-HT(3A) receptor-bearing white matter interstitial GABAergic interneurons are functionally integrated into cortical and subcortical networks. *J Neurosci* **31**, 16844–16854.

von Monakow C (1905) *Gehirnpathologie*. Wien: Alfred Holder.

Wahle P, Meyer G (1987) Morphology and quantitative changes of transient NPY-ir neuronal populations during early postnatal development of cat visual cortex. *J Comp Neurol* **261**, 165–192.

Wegiel J, Flory M, Kuchna I, et al. (2014) Stereological study of the neuronal number and volume of 38 brain subdivisions of subjects diagnosed with autism reveals significant alterations restricted to the striatum, amygdala and cerebellum. *Acta Neurophatol Comm* **2**, 141.

West MJ, Gundersen HJ (1990) Unbiased stereological estimation of the number of neurons in the human hippocampus. *J Comp Neurol* **296**, 1–22.

Žunić Išasegi I, Radoš M, Krsnik Ž, et al. (2018) Interactive histogenesis of axonal strata and proliferative zones in the human fetal cerebral wall. *Brain Struct Funct* **223**, 3919–3943.